Available online at www.sciencedirect.com
ScienceDirect
Communications in Nonlinear Science and Numerical Simulation xxx (2007) xxx–xxx
Communications in Nonlinear Science and Numerical Simulation
www.elsevier.com/locate/cnsns

Dynamics of transport under random fluxes on the boundary

Vena Pearl Boñgolan-Walsh [a,*], Jinqiao Duan [a], Tamay Özgökmen [b]

[a] Department of Applied Mathematics, Illinois Institute of Technology, Chicago, IL 60616, USA
[b] Rosenstiel School of Marine and Atmospheric Science, Meteorology and Physical Oceanography Division (RSMAS, MPO), University of Miami, Miami, FL 33149-1098, USA

Received 19 July 2005; received in revised form 19 March 2006; accepted 1 September 2006

Abstract

The impact of boundary noise on the dynamical evolution of the scalar transport equation in shear flows is studied, taking off from earlier studies in shear-flow dispersion in internal waves, a mechanism for horizontal mixing in the ocean. In particular, we model a gravity current evolving under an assumed shear-flow. The transport equation is deterministic, with a noise term at the inlet *boundary*. This was motivated by observed seasonal fluctuations in some known sources of salty, dense water in the oceans, like the Red Sea overflow, as well as observed thermal and saline anomalies in the thermohaline circulation.

The noises used were: Wiener white, Wiener colored, Lévy white, and Lévy colored noise. Lévy processes form a more general class of processes which are generally non-Gaussian in distribution, and may have infinitely many jumps in finite time. They have been used to model pollutant point-sources, the flight time of particles in vortices, and linear and nonlinear anomalous diffusion.

The major finding was that white noises (Wiener and Lévy) and colored Wiener noise all have the effect of impeding the diffusion process, by as much as 33%. However, colored Lévy noise (non-Gaussian, time-correlated) does not have this effect on diffusion. This would suggest that time-correlation is more important in distinguishing noises than the distribution of the process that produced the noise. This also explains why Lévy colored noise showed great sensitivity to the stability parameter α, while Lévy white noise is unaffected by its stability parameter.
© 2007 Published by Elsevier B.V.

PACS: 92.60.Ek; 02.50.Ey; 02.60.Cb

Keywords: Scalar transport equation; Stochastic boundary conditions; Numerical simulations

1. Introduction

There is a growing recognition of a role for the inclusion of stochastic terms in the modelling of complex systems. As an example, there has been increasing interest in mathematical modelling via stochastic partial

* Corresponding author. Tel.: +1 312 567 5337; fax: +1 312 567 3135.
E-mail address: bongven@iit.edu (V.P. Boñgolan-Walsh).

1007-5704/$ - see front matter © 2007 Published by Elsevier B.V.
doi:10.1016/j.cnsns.2006.09.019

Please cite this article in press as: Boñgolan-Walsh VP et al., Dynamics of transport under random fluxes on the boundary, Commun Nonlinear Sci Numer Simul (2007), doi:10.1016/j.cnsns.2006.09.019

UNCORRECTED PROOF

differential equations (SPDEs), for the climate system, condensed matter physics, materials sciences, mechanical and electrical engineering, and finance. The addition of stochastic terms has led to interesting new mathematical problems at the interface of dynamical systems, partial differential equations, scientific computing, and probability theory. Problems arising in the context of stochastic dynamical modelling have inspired interesting research topics like the interaction between noise, nonlinearity and multiple scales, and about efficient numerical methods for simulating random phenomena.

Sometimes, noise affects nonlinear systems at the boundary. *Static* boundary conditions, such as Dirichlet or Neumann boundary conditions, do not involve time derivatives of the unknowns. The transport equation used is deterministic, with a noise term at the inlet *boundary*. This was motivated by several observations, like the seasonal variability of the Red Sea overflow (a source of salty, dense water flowing into the Gulf of Aden) [1], and it is a static random Neumann boundary condition [2]. Systems under static random boundary conditions have been studied recently in, for example [3–6]. In addition, there have been observed thermal and saline anomalies in the thermohaline circulation, e.g. [7]. However, this latter study had the anomalies as added scalar terms in the heat and transport equations.

In most studies, Wiener *white* noise is used as the model for noise because of its simplicity, i.e., Gaussian in distribution, and uncorrelated in time. However, Wiener white noises cannot be realized physically, and are, in fact, approximated by their conventional, broad-banded counter-parts, colored noises [8]. In this paper, we extend those studies to include colored (time-correlated) noises, which are solutions to a linear Ornstein–Uhlenbeck stochastic equation, and would be closer to what is observed in nature.

Furthermore, this study explores noise produced by Lévy processes, a more general class of processes which includes Wiener processes. Lévy processes are, in general, non-Gaussian in distribution, and more importantly, they may have infinitely many jumps in finite time, subject to the integrability condition. These have long been used in financial applications, and are now also used in the physical sciences. Wolpert in [9] used Lévy random fields to model pollutant point-sources, and Lévy processes serve as their prior distribution for the pollutant levels. Woyczynski in [10] used Lévy processes to study flight time of particles in vortices, and linear and nonlinear anomalous diffusion.

The noises used were:

Wiener white noise: $\dot{W}_t$, which is the formal derivative of W_t, a Brownian motion or Wiener process. This is usually called Gaussian white noise, but since Lévy processes could also produce white noise, we will avoid confusion by referring instead to the process that produced the noise, hence we call it Wiener white noise. In the literature, W_t is sometimes written $W(t)$; this subscripted notation does *not* denote differentiation with respect to time.

Wiener colored noise: η_t, which has time-correlated covariance (*colored*), and which satisfies a linear Ornstein–Uhlenbeck stochastic differential equation driven by $\dot{W}_t$.

Lévy white noise: $\dot{L}_t$, where L_t is a Lévy motion; L_t may or may not have a Gaussian distribution. Just like Wiener white noise, the covariance is not time-correlated.

Lévy colored noise: v_t, which has time-correlated covariance (*colored*), and which also satisfies a linear Ornstein–Uhlenbeck stochastic differential equation driven by $\dot{L}_t$. Again, L_t need not have a Gaussian distribution.

We distinguish Lévy noises by their index of stability α, which in turn determines the distribution for the process, viz., $\alpha = 2$ means the processes have a Gaussian distribution, $\alpha = 1$ means a Cauchy distribution, and α values in between are referred to as Lévy noises.

The effects of these noises were studied by numerical simulations using a finite element method. Aside from observing $S(x,z,t)$, the averaged tracer or passive scalar value of a current at time t, we also took differences in the averaged tracer values, e.g., $|S(x,z,t)_{\text{deterministic}} - S(x,z,t)_{\text{with noise}}|$.

2. Scalar transport equation with random boundary fluxes

Consider a passive scalar (also called *tracer*) $S = S(x,z,t)$. S may be taken to be temperature, salinity or concentration of a chemical specie. Assuming the velocity field $u(x,z,t)$ is known from the fluid momentum equations (u is divergence-free and no-slip on boundary),

$$S_t + u \cdot \nabla S = \kappa \Delta S, \quad (x,z) \in D \tag{1}$$

Please cite this article in press as: Boñgolan-Walsh VP et al., Dynamics of transport under random fluxes on the boundary, Commun Nonlinear Sci Numer Simul (2007), doi:10.1016/j.cnsns.2006.09.019

UNCORRECTED PROOF

where $D = [0,1] \times [0,1]$, and $\kappa > 0$ is the salute diffusivity.

Young et al. [11] modelled advection–diffusion in the oscillatory, sheared-velocity field of an internal wave, by assuming $u = \beta t \cos(\omega t)$, or a variant with sinusoidal vertical structure, $u = u_0 \cos(mz)\cos(\omega t)$. We likewise assume a known velocity field here.

This linear transport equation is then supplemented with the following boundary conditions:

$$\begin{aligned} &\frac{\partial S}{\partial n} = F(z) + \text{noise, on inlet boundary,} \quad x = 0 \\ &\frac{\partial S}{\partial n} = 0 \text{ on rest of boundary} \end{aligned} \tag{2}$$

where $F(z)$ is the mean tracer or passive scalar flux. In the case of Wiener white noise, $\frac{\partial S}{\partial n} F(z) + \dot{W}_t$, where W_t is a Brownian motion defined in a probability space $(\Omega, \mathscr{F}, \mathbb{P})$.

A form for the solution is known, using a theorem of Da Prato and Zabczyk [4]. If we let A be the linear (in S) operator

$$A = -u \cdot \nabla - \kappa \Delta \quad (x,z) \in D \tag{3}$$

then the equation has the form

$$S_t = AS \tag{4}$$

and we write the boundary conditions as a vector Y

$$Y = \begin{pmatrix} F(z) + \dot{W}_t \\ 0 \end{pmatrix}, \tag{5}$$

we may let operator γ define the boundary conditions as

$$\gamma S = Y \tag{6}$$

Here, we will just assume that A generates a C_0 semigroup of operators $X(t)$, $t \geqslant 0$. A proper proof will require verification of the requirements of the Lumer–Philipps theorem.

If we designate as

$$\mathscr{N}(Y) = \phi \tag{7}$$

where

$$A(\lambda - \phi) = 0 \tag{8}$$

that is, $\mathscr{N}$ is the solution operator of the above eigenvalue problem, then we write the solution as

$$S = X(t)S_0(x,z) + (\lambda - A)\int_0^t X(t-s)\mathscr{N}(Y)\,\mathrm{d}s \tag{9}$$

3. Numerical simulations via finite element method

In our numerical simulations, we made use of a finite-element Fokker–Plank solver developed at Clemson University by Prof. Vince Ervin. The domain is a 16×16 triangularization of the square $[0,1] \times [0,1]$. This solves the transport equation for a tracer $S(x,z,t)$ on a rectangular domain, under flux (Neumann) boundary condition.

$$S_t + v \cdot \nabla S + qS = \nabla(\kappa \cdot \nabla S), \tag{10}$$

where $\kappa > 0$ is the salute diffusivity, and v is a given function of velocity. For our problem, q is zero (no reaction term).

Here $\kappa = .01$ was assumed constant throughout the domain. This was chosen to 'slow-down' the diffusion process and allow the gravity current to evolve during our simulation time.

Please cite this article in press as: Boñgolan-Walsh VP et al., Dynamics of transport under random fluxes on the boundary, Commun Nonlinear Sci Numer Simul (2007), doi:10.1016/j.cnsns.2006.09.019

UNCORRECTED PROOF

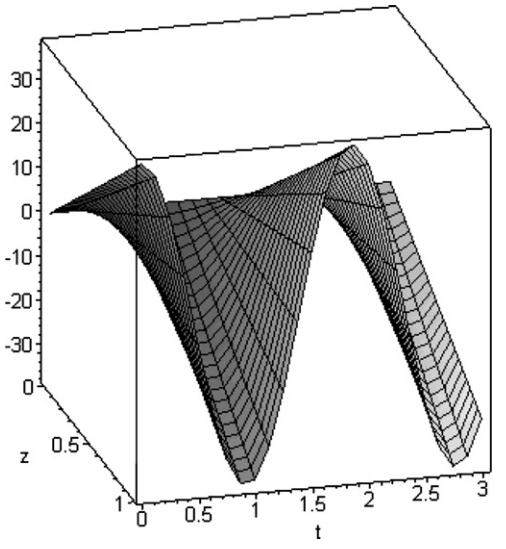

Fig. 1. Velocity field as a function of z and t.

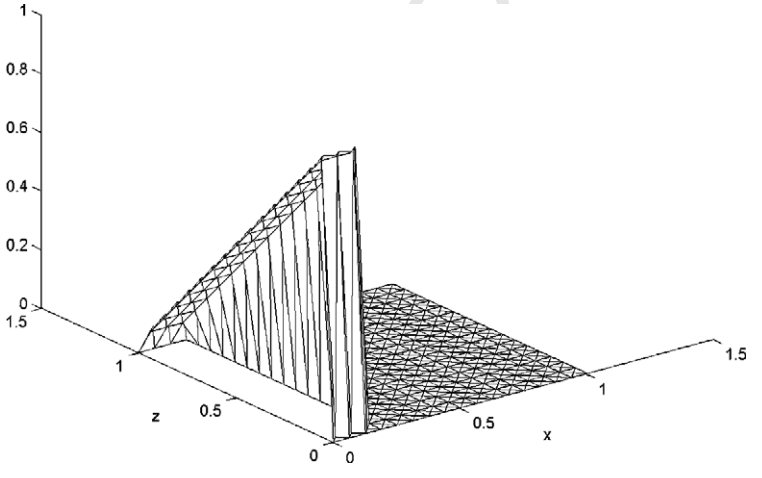

Fig. 2. $S(x,z,0)$, initial values of tracer.

Young et al. [11] assumed velocity fields like $u = \beta t\cos(\omega t)$ or $u = u_0\cos(mz)\cos(\omega t)$. In this study, we likewise assumed an oscillatory shear flow v in the x (downstream) direction, zero in the vertical (z) direction, The x-component has the form

$$v = 0.5z\cos(\omega t) \times \text{scaling}, \tag{11}$$

where scaling ($presently = 75$) is used to control the speed of the current, just so it will not go over the right boundary in our simulation time. See Fig. 1 for a plot of the x-component of velocity as a function of z (vertical direction) and time t.

Time-stepping was by the backward-Euler method.

Fig. 2 shows the initial distribution of the tracer or passive scalar in the domain, or $S(x,z,0)$. This is similar to the assumed salinity distribution in gravity current studies done by Özgökmen et al. in [12] and by Boñgolan-Walsh et al. in [13]. Fig. 3 shows the color density plot for the initial salinity distribution in those exper-

Please cite this article in press as: Boñgolan-Walsh VP et al., Dynamics of transport under random fluxes on the boundary, Commun Nonlinear Sci Numer Simul (2007), doi:10.1016/j.cnsns.2006.09.019

Fig. 3. Color-density plot of initial values for salinity.

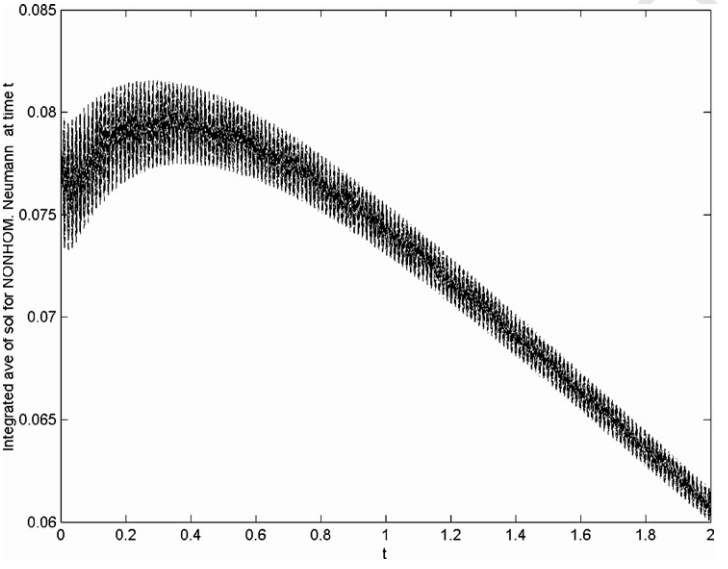

Fig. 4. Averaged tracer value at time t for a gravity current evolving under deterministic, non-homogenous Neumann boundary conditions.

iments. Note that, in both presentations, the highest salinity is at $z = 0$ (shown as red[1] in the color-density plot), and steadily goes to zero as z goes to 1 (blue). The present experiment assumed a linear decrease, while the experiments in [13,12] assumed an exponential decrease.

3.1. Deterministic case

In the simulations following, we assumed $F = 1$ in the boundary condition $F(z) + \text{noise}$. Thus, the comparison base case is a non-homogenous Neumann boundary condition, which could represent the average flux for the tracer, which we later perturb with noise.

Fig. 4 plots the averaged scalar value for the entire domain at time t, i.e., $S(x, z, t)$. Since the equation is one of diffusion, we see the averaged value of the tracer (e.g., salinity or temperature) steadily decreasing with time. A close inspection of the graph shows this happens in an oscillatory manner, even *without* noise.

Later experiments will show how this diffusion process is affected by different kinds of boundary noises and shear flow velocity (which is assumed to be a cosine function). Specific to Lévy noise, we will also see how the index of stability α affects this diffusion.

The scaling factor used in the shear-flow velocity in (11), and the salute diffusivity κ, in (10), were fine-tuned so as to give a current that would reach the outlet at about 2000 time-steps, at the same time avoiding wild, unphysical fluctuations in the tracer or passive scalar distribution, e.g., some combinations we tried would show some part of the gravity current having negative values for the tracer.

[1] For interpretation of color in Fig. 3, the reader is referred to the web version of this article

Please cite this article in press as: Boñgolan-Walsh VP et al., Dynamics of transport under random fluxes on the boundary, Commun Nonlinear Sci Numer Simul (2007), doi:10.1016/j.cnsns.2006.09.019

At each time-step, the tracer was averaged via

$$\text{Average} = \frac{\int_{\text{triangle}} S\,\mathrm{d}x\,\mathrm{d}z}{\text{area of triangle}} \tag{12}$$

where the integral is over each triangle in the spatial discretization. The values from all triangles in the domain were then averaged, giving the average value for the entire current at time t. This averaged value is what is being graphed in Fig. 4.

Fig. 5 shows the values of the tracer at $t = 130$. Comparing it with the initial distribution in Fig. 2, one sees that the distribution of the tracer (e.g., salinity) quickly diffuses over the domain. This diffusion is also seen in Fig. 4, with the decrease in averaged values.

3.2. White noises on inlet boundary

Wiener white noise $\dot{W}_t(\omega)$ is the formal derivative of a Brownian motion W_t, which may be regarded as a solution of the simplest (linear) stochastic differential equation

$$\dot{W}_t(\omega) = \frac{\mathrm{d}W_t}{\mathrm{d}t} \tag{13}$$

There is, however a more general class of noises which may also be taken to be 'white' in the sense they are uncorrelated in time. However, their distribution need not be Gaussian. We begin with the definition in Applebaum [14]: Given a probability space $(\Omega, \mathscr{F}, \mathscr{P})$. A Lévy y process $(L_t, t \geqslant 0)$ taking values in $\mathbb{R}^d$ is a stochastic process having stationary and independent increments; we always assume that $L_0 = 0$ with probability of one.

However, Lévy processes L_t are defined in terms of their characteristic function, viz

$$\mathbb{E}(\mathrm{e}^{\mathrm{i}(u,L_t)}) = \mathrm{e}^{tg(u)} \tag{14}$$

where

$$g(u) = \mathrm{i}(b,u) - \frac{1}{2}(u,au) + \int_{\mathbb{R}^d-\{0\}} (\mathrm{e}^{\mathrm{i}(u,y)} - 1 - \mathrm{i}(u,y)\chi_{0<|y|<1}(y))\mathbf{m}(\mathrm{d}y). \tag{15}$$

This is the famous Lévy–Khintchine formula, and from here we see that Lévy processes encompasses familiar processes. If, say $a = \mathbf{m} = 0$, we have $L_t = bt$ which is deterministic motion in a straight line, where b is the velocity of motion, or the *drift*. On the other hand, if $a \neq 0$, $\mathbf{m} = 0$, then L_t is a Brownian motion with drift, since the formula gives us the characteristic function of a Gaussian random variable with mean tb and covariant matrix ta.

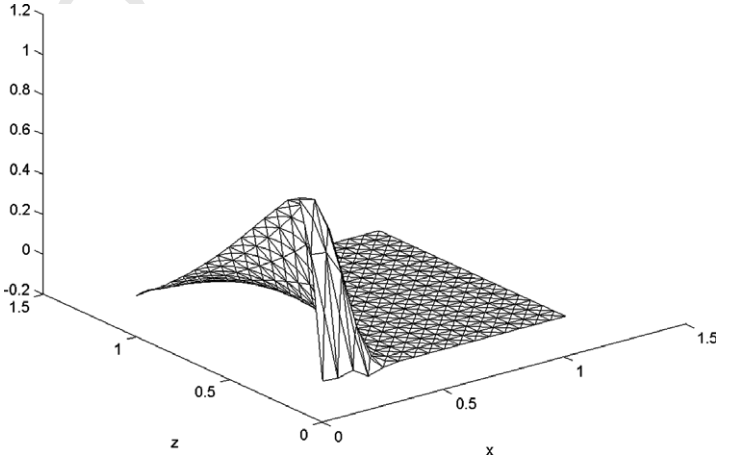

Fig. 5. $S(x,z,130)$, values of tracer at $t = 130$.

Please cite this article in press as: Boñgolan-Walsh VP et al., Dynamics of transport under random fluxes on the boundary, Commun Nonlinear Sci Numer Simul (2007), doi:10.1016/j.cnsns.2006.09.019

Our interest is when $\mathbf{m} \neq 0$, but is a finite measure, say $\mathbf{m} = \lambda\delta_h$, where $\lambda > 0$ and δ_h is a Dirac mass at $h \in \mathbb{R}^d - [0]$. In this case, we can set $L_t = b't + \sqrt{(a)}B_t + N_t$, where B_t is a standard Brownian motion, and N_t is a Poisson process of intensity λ taking values in the set $\{nh, n \in \mathbb{N}\}$.

Physically, we might interpret this as: L initially follows a path of a Brownian motion with drift until random time T_1, at which time the path has a jump discontinuity of size $|h|$. It then returns to Brownian motion until time T_2, when it again undergoes a jump discontinuity of the same size $|h|$.

We may generalize the measure $\mathbf{m}$ to $\mathbf{m} = \sum_{i=1}^{m} \lambda_i \delta_{h_i}$. Then, the motion is still Brownian with drift, interspersed with jumps, but now the jump sizes are variable, and may be any of the numbers $|h_1|$, $|h_2|$, etc.

However, for our numerical simulations, we use α-stable Lévy motions defined in Janicki and Weron [15]. See also [16].

This is a particular form of the Lévy–Khintchine formula. Here L_t is a stochastic process having independent increments, and we also assume that $L_0 = 0$ with probability of one. Now, we assume $L_t - L_s \sim G_\alpha((t-s)^{\frac{1}{\alpha}}, \beta, 0)$ for any $0 \leqslant s < t < \infty$.

The general symbol for an α-stable random variable is $G_\alpha(\sigma, \beta, \mu)$. Its characteristic function is given by

$$\log \phi(\theta) = -\sigma^\alpha |\theta|^\alpha (1 - \mathrm{i}\beta \mathrm{sgn}(\theta) \tan(\alpha\pi/2)) + \mathrm{i}\mu\theta \tag{16}$$

where α is called the index of stability $\alpha \in (0,1) \bigcup (1,2]$; β is the skewness, and $\beta \in [-1,2]$; σ is called the scale parameter (this is simply standard deviation when $\alpha = 2$), and $\sigma \in \mathbb{R}_+$, and μ is the shift (mean) of the distribution, $\mu \in \mathbb{R}$.

We transcribed the computer simulation provided by Janicki and Weron for the class of processes $G_\alpha(1,0,0)$. When α is 2, the resulting motion is Brownian, and the distribution is in fact Gaussian! Away from $\alpha = 2$, the distribution is no longer Gaussian, and this provides a very interesting class of motions which include Cauchy motion (when $\alpha = 1$), and Lévy motion when α is any other number in $(0,2)$.

3.3. Colored noises on inlet boundary

We consider the colored noise $\eta_t(\omega)$ as a solution of a (linear) Ornstein–Uhlenbeck stochastic equation

$$\eta_t = -\beta\eta + \alpha\frac{\mathrm{d}W_t}{\mathrm{d}t} \tag{17}$$

where $\frac{\mathrm{d}W_t}{\mathrm{d}t} = \dot{W}_t$ is Wiener white noise. The solution $\eta_t(\omega)$ has time-correlated covariance (and thus is used as a model for colored noise). We solved this via Milstein's Method, see [8].

We modelled Lévy colored noise similarly, except that the term $\frac{\mathrm{d}W_t}{\mathrm{d}t}$ is replaced now by Lévy white noise $\frac{\mathrm{d}L_t}{\mathrm{d}t}$, so

$$v_t = -\beta v + \alpha\frac{\mathrm{d}L_t}{\mathrm{d}t} \tag{18}$$

Janicki and Weron generalized the Milstein method to include Lévy processes in Chapters 6 and 8 of [15].

4. Results

4.1. Effects on the diffusion process

Taking $\alpha = 1.5$ as our 'standard' stability index for a Lévy process, we conducted experiments with Wiener noises (white and colored), and Lévy ($\alpha = 1.5$) noises (white and colored) on the boundary. Currents evolving under noise conditions were first compared with the deterministic*base* case, which assumes non-homogenous Neumann boundary conditions.

Fig. 6 shows the averaged values at time t for the case of Wiener White noise at the boundary. Comparing it with Fig. 4 (base case), we see that Wiener White noise has the effect of delaying the diffusion process, resulting in a higher averaged value of about $\overline{S} = 0.08$ by the end of the simulation ($t = 2000$), whereas the deterministic base case gives an averaged value of 0.06, for a difference of about 33%. Experiments with Wiener colored and Lévy white noises showed the same result, a 33% difference in the final average value for the tracer.

UNCORRECTED PROOF

Please cite this article in press as: Boñgolan-Walsh VP et al., Dynamics of transport under random fluxes on the boundary, Commun Nonlinear Sci Numer Simul (2007), doi:10.1016/j.cnsns.2006.09.019

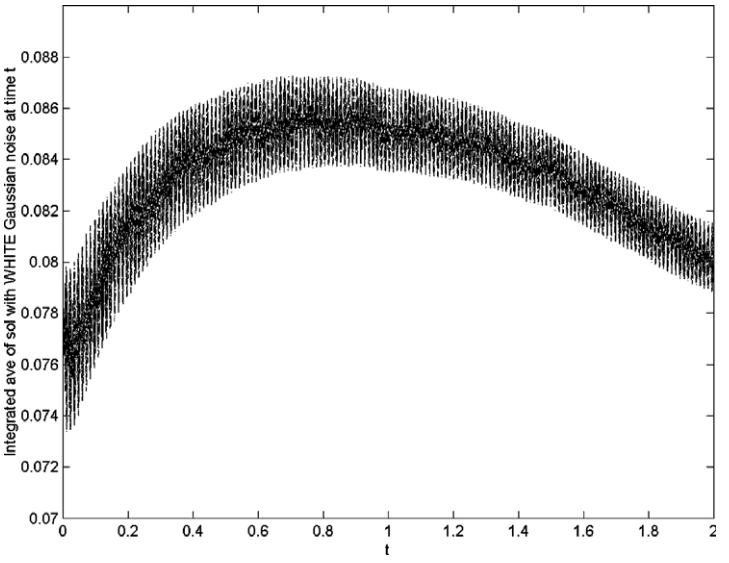

Fig. 6. Averaged tracer value at time t for a gravity current evolving with Wiener white noise in the boundary.

Fig. 7 shows the averaged values for Lévy colored noise. This shows an ending average value close to that of the Wiener white noise, suggesting the over-all diffusion is not affected. However, this does not mean that it is not a 'strong' noise, in the sense that it has no effect on the current, as the next section shows.

Another way of comparing currents evolving under different noise processes is to take the absolute value of the difference in the tracer values from the deterministic base case, i.e., $|S(x,z,t)_{\text{deterministic}} - S(x,z,t)_{\text{with noise}}|$. Fig. 8 graphs the magnitude of the absolute differences in scalar in each current against the index of stability (α) used.

Since Wiener noises are independent of α, they are constant throughout. Note however, that white and colored Wiener noises have *identical* effects on the average value of the tracer in evolving currents, suggesting that time-correlation in Wiener noise processes has no effect on the average diffusion of the tracer. We note too that

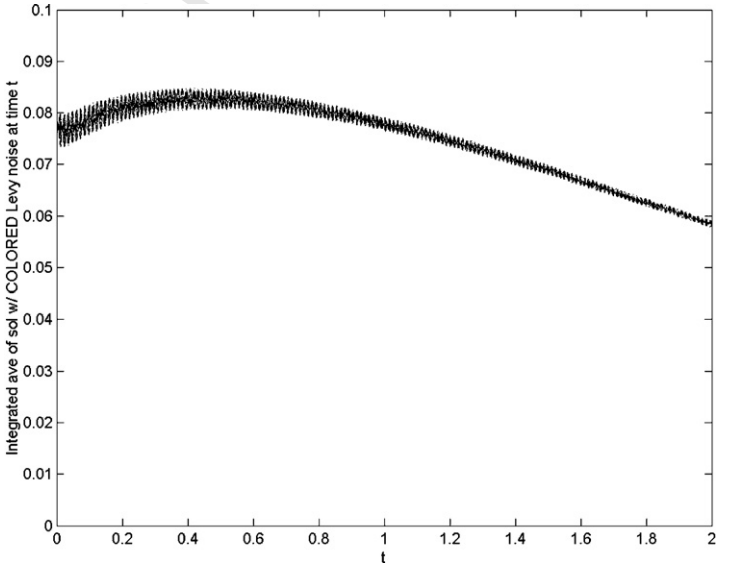

Fig. 7. Averaged tracer value at time t for a gravity current with Levy colored noise in the boundary.

Please cite this article in press as: Boñgolan-Walsh VP et al., Dynamics of transport under random fluxes on the boundary, Commun Nonlinear Sci Numer Simul (2007), doi:10.1016/j.cnsns.2006.09.019

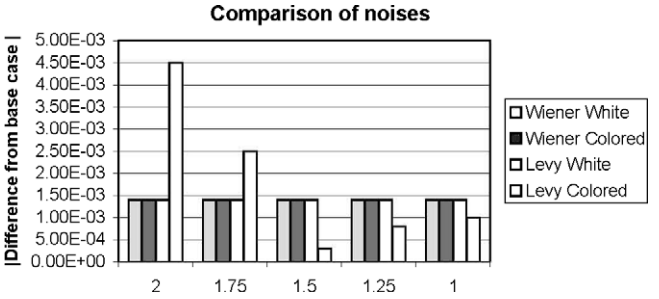

Fig. 8. Magnitude against α for Levy noise.

Lévy white noise has the same effect as both Wiener noises, i.e., their developing currents all have the same averaged differences in tracer values from the deterministic base case, and we earlier noted that they all have the effect of delaying or impeding the diffusion process.

4.2. Sensitivity of lévy colored noise to α

Now we concentrate on currents developing with Lévy colored noise on the boundary. In the previous section, we saw that these currents exhibited great sensitivity to the index of stability α. Using the metric $|S(x,z,t)_{\text{deterministic}} - S(x,z,t)_{\text{with Levy colored noise}}|$, Figs. 9–13 show plots of this difference for several values α.

Figs. 9–11 all show a start-up, or transient period, then the effects of the noise increase almost linearly with time. These figures show that the start-up period increases with decreasing α, from less than 300 seconds when $\alpha = 2$, to about 1400 s for $\alpha = 1.5$. Since the index of stability α actually refers to the distribution of the processes, with $\alpha = 2$ being Gaussian-distributed, and $\alpha = 1.5$ being Lévy-distributed, this tells us that the noises produced by Gaussian and almost Gaussian-distributed processes act slower than their non-Gaussian or Lévy counterpart.

We see from Figs. 11–13 the jumps characteristic of non-Gaussian Lévy processes, becoming most pronounced when the distribution is Cauchy. Note too that, in all three cases, after the start-up period, the increasing part of the curve is concave, suggesting a continuous growth in the differences.

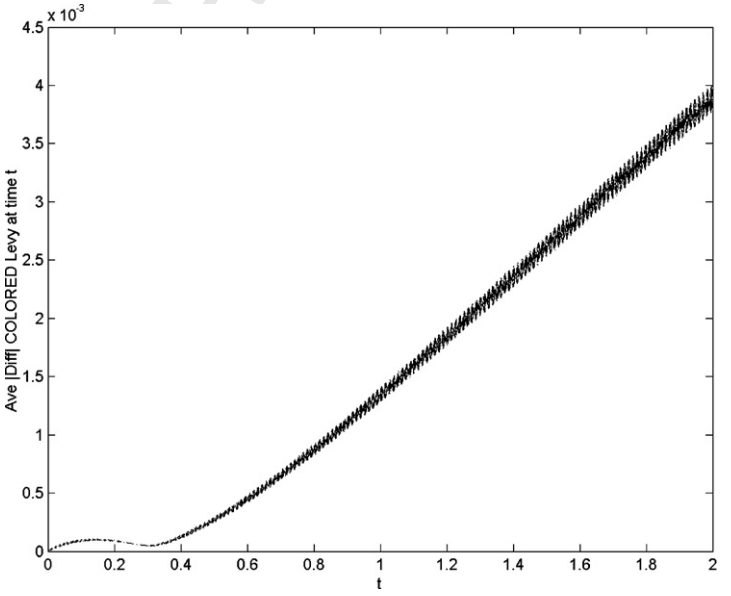

Fig. 9. Difference from base case, $\alpha = 2$ (Gaussian).

Please cite this article in press as: Boñgolan-Walsh VP et al., Dynamics of transport under random fluxes on the boundary, Commun Nonlinear Sci Numer Simul (2007), doi:10.1016/j.cnsns.2006.09.019

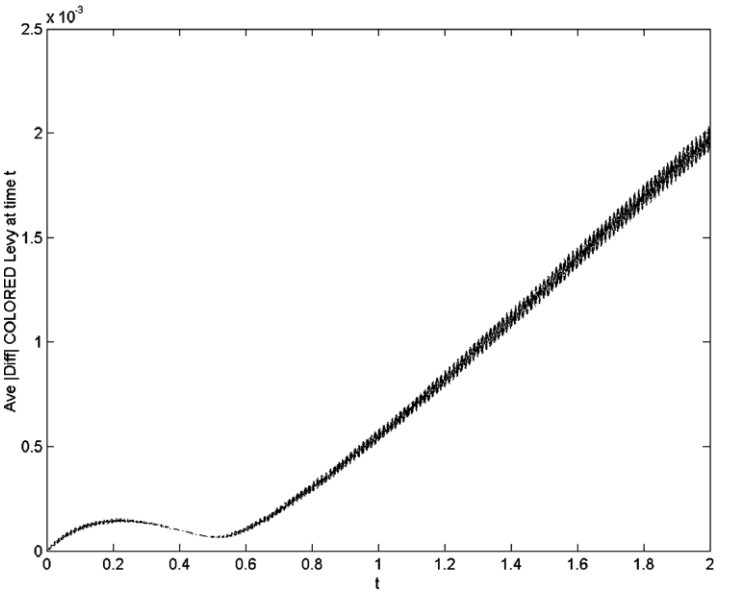

Fig. 10. Difference from base case, $\alpha = 1.75$ (Levy).

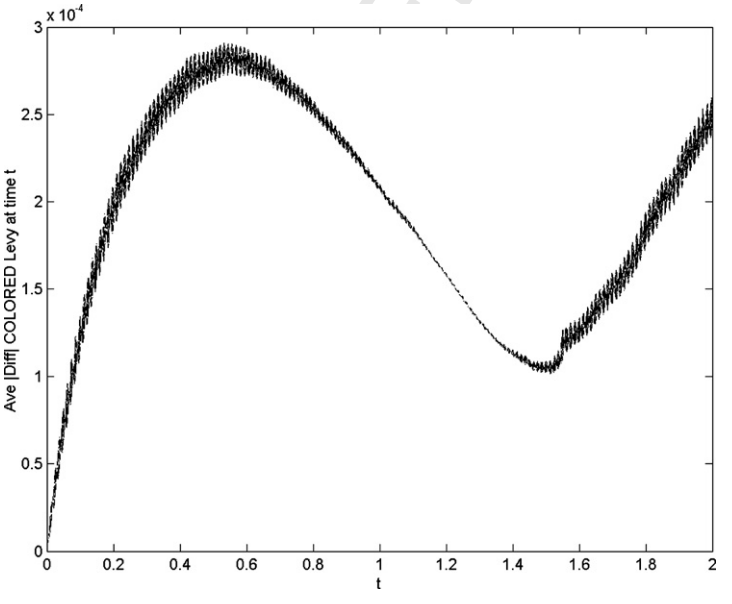

Fig. 11. Difference from base case, $\alpha = 1.5$ (Levy).

Figs. 12 and 13 are for $\alpha = 1.25$ and $\alpha = 1.0$. These are already far from Gaussian, and are heading towards the Cauchy distribution. Notice now that the graphs show a learning-curve, i.e., the differences seem to be asymptotic to some limiting value.

It is also worth noting that, as α goes from 2 to 1.5, there is a marked *decrease* in the magnitude of the differences, from 4.5×10^{-3} for $\alpha = 2$, to 3×10^{-4} for $\alpha = 1.5$. On the other hand, as α goes from 1.5 to 1, we see an *increase* in the magnitude of the differences, from 3×10^{-4} for $\alpha = 1.5$ to 1×10^{-3} for $\alpha = 1.0$.

Please cite this article in press as: Boñgolan-Walsh VP et al., Dynamics of transport under random fluxes on the boundary, Commun Nonlinear Sci Numer Simul (2007), doi:10.1016/j.cnsns.2006.09.019

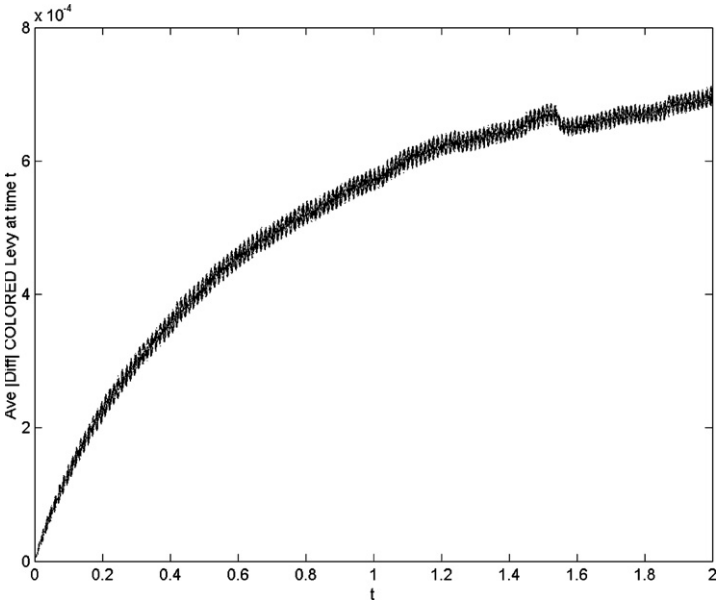

Fig. 12. Difference from base case, $\alpha = 1.25$ (Levy).

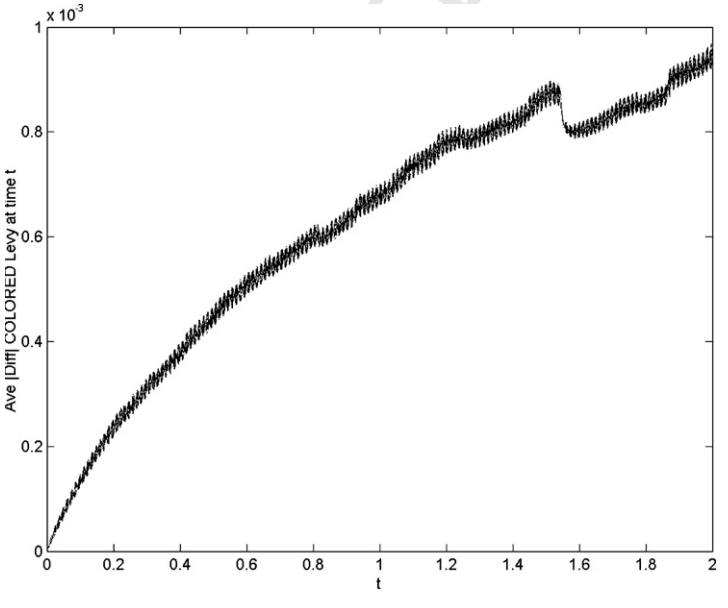

Fig. 13. Difference from base case, $\alpha = 1.0$ (Cauchy).

4.3. Comparing colored noises

From the previous sections, it was already seen that white noises behave similarly, i.e., there was no difference in the effects of Wiener white noise and Lévy white noise on an evolving current, regardless of the α value used for Lévy noise.

With the colored noises, however, the finding is that, at $\alpha = 2$, the difference in tracer values between the developing currents was of the order 0.09, but this decreases dramatically to an order of 0.005 as α goes to 1. Figs. 14–16 show what is happening from $\alpha = 1.5$ to $\alpha = 1$. We see a decrease in the magnitude of the differ-

Please cite this article in press as: Boñgolan-Walsh VP et al., Dynamics of transport under random fluxes on the boundary, Commun Nonlinear Sci Numer Simul (2007), doi:10.1016/j.cnsns.2006.09.019

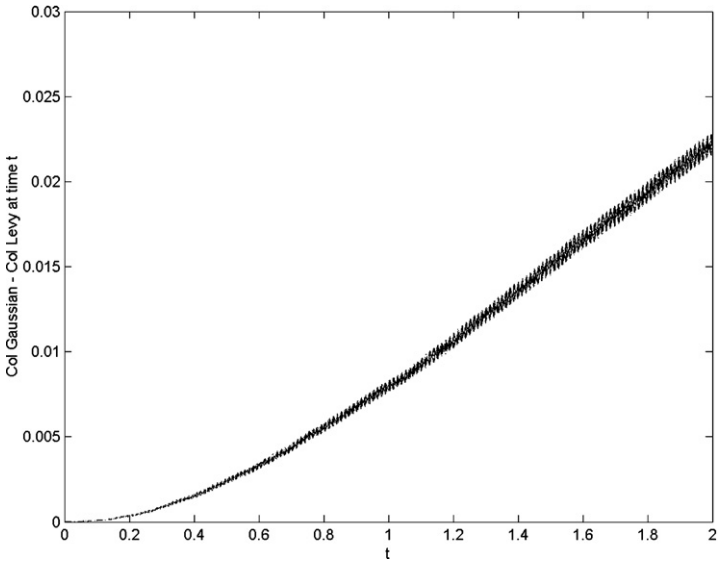

Fig. 14. Wiener noise – Levy noise, $\alpha = 1.5$.

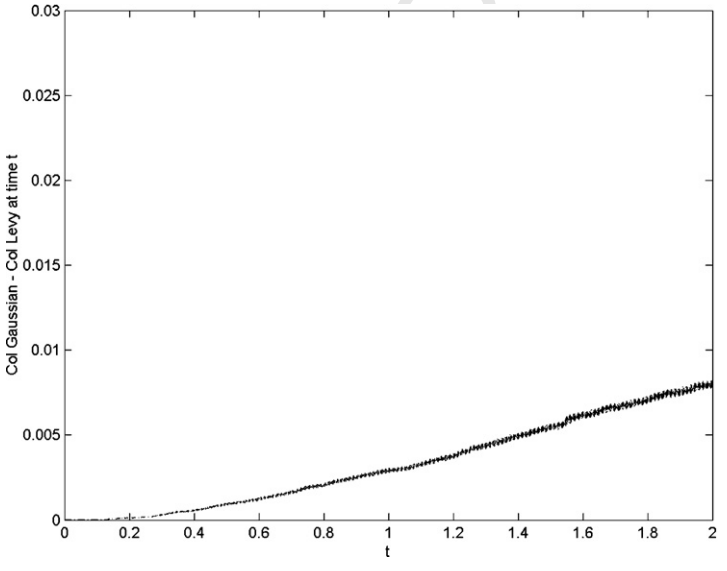

Fig. 15. Wiener noise – Levy noise, $\alpha = 1.25$.

ences, and we also see jumps developing in the graph, which correspond to jumps in the tracer values for Lévy colored noise.

4.4. Impact of varying the period of velocity

Recall the x-component of the velocity vector for our shear flow: $v = 0.5z\cos(\omega t) \times$ scaling, with the y-component being zero. We took as a 'normal' period (ω) as one phase of the cosine function from initial time to final time. The experiment here varied the period or ω in the expression for v above.

First, the period was tripled, from $\omega = 1$ to $\omega = 3$, and the resulting graphs of the average tracer were compared. This experiment should have affected all of the cases, i.e., the deterministic base case and with noises added. However, the solutions turned out to be quite robust relative to the shear velocity, since there was very

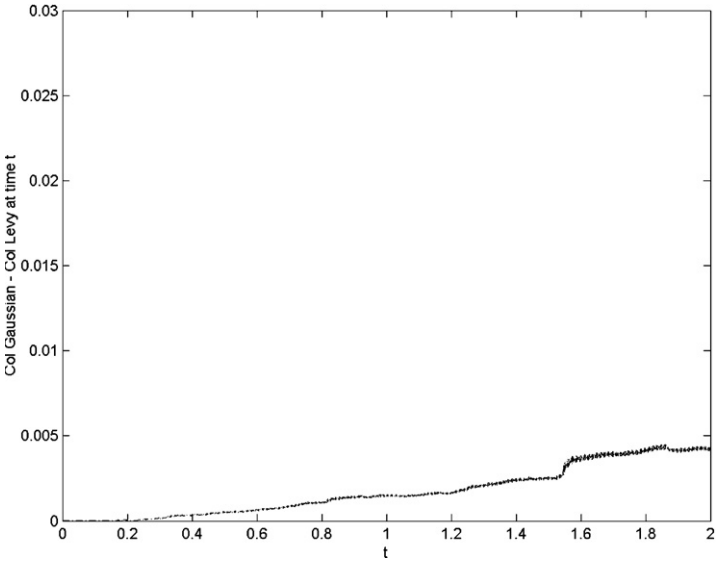

Fig. 16. Wiener noise – Levy noise, $\alpha = 1.0$.

little qualitative change in the averaged values of the tracer from $\omega = 1$ to $\omega = 3$. This held true for the deterministic case, and all the cases with noise.

There was also little quantitative impact. It was previously noted that the graphs of the average tracer show oscillations as the current evolved, e.g., Fig. 4. There was a slight change in the amplitudes of these oscillations: the deterministic case (non-homogenous Neumann) decreased slightly to 0.925 of normal, while the oscillations for white Wiener noise increased slightly to 1.14 of normal.

There was, however, a big impact in dividing the period by three (giving the shear flow a higher frequency). The amplitudes of the oscillations increased noticeable, with colored Lévy showing about twice the normal amplitude, white Wiener about 1.9 times normal, white Lévy and colored Wiener both about 1.86 times normal, The smallest effect was for the deterministic, comparison case, only 1.5 times normal.

Figs. 17–19 show the integrated averages of tracer value for currents developing with White Lévy noise on the boundary. These suggest that a higher-frequency shear flow locally 'magnifies' the diffusion process, but

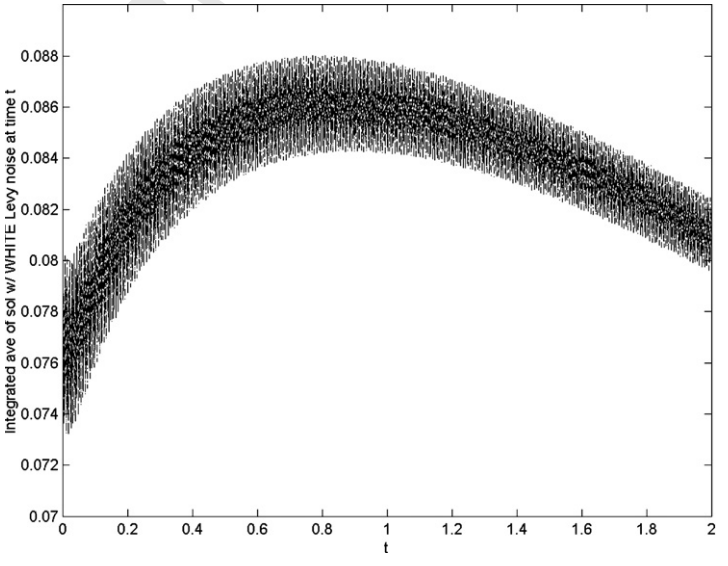

Fig. 17. Averaged tracer value with white Levy noise at the boundary, period tripled.

Please cite this article in press as: Boñgolan-Walsh VP et al., Dynamics of transport under random fluxes on the boundary, Commun Nonlinear Sci Numer Simul (2007), doi:10.1016/j.cnsns.2006.09.019

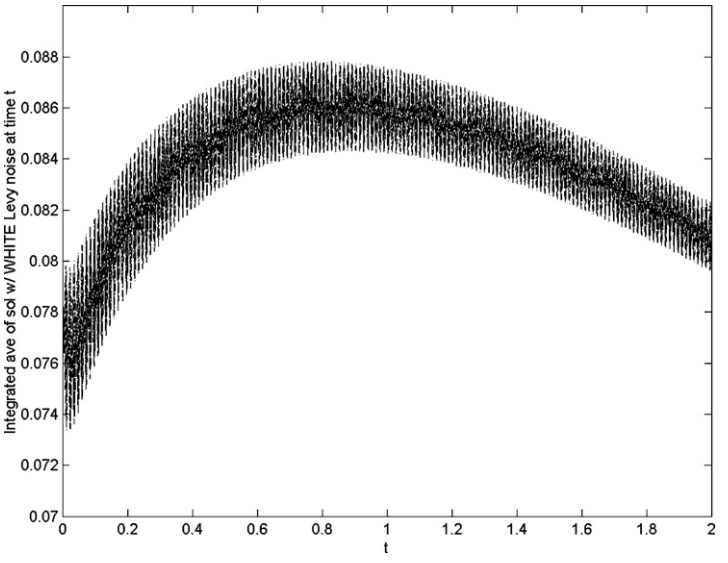

Fig. 18. Averaged tracer value with white Levy noise at the boundary, normal period.

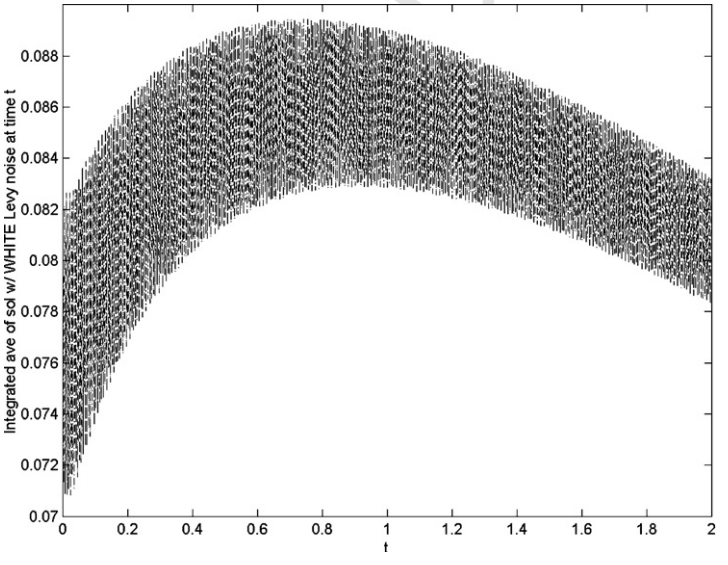

Fig. 19. Averaged tracer value with white Levy noise at the boundary, one third period.

since the behavior is oscillatory about a mean value, there is no noticeable effect in the over-all diffusion. Note the three currents have roughly the same average value for the scalar at the end of the simulation.

The same trend was observed across all cases, i.e., the deterministic base case, Wiener and Lévy noises, white or colored.

5. Summary

Comparisons were made among currents evolving under deterministic boundary conditions (non-homogenous Neumann) and with a stochastic term added to the boundary, viz: Wiener white and colored noises and Lévy white and colored noises.

Please cite this article in press as: Boñgolan-Walsh VP et al., Dynamics of transport under random fluxes on the boundary, Commun Nonlinear Sci Numer Simul (2007), doi:10.1016/j.cnsns.2006.09.019

Both Wiener noises (white and colored), and white Lévy noise all had the effect of delaying the diffusion process, producing a current that was 33% more saline. These three boundary conditions gave a higher average value for the tracer, $\overline{S} = 0.08$, compared to 0.06 for the deterministic base case. Colored Lévy noise, gave the same ending averaged value as the deterministic case, $\overline{S} = 0.06$.

However, it is Lévy colored noise which showed the greatest sensitivity to the stability parameter α. Qualitatively, closer to $\alpha = 2$, we see a start-up or transient period in the graph of the differences, and a continuous increase in the strength of the noise; closer to $\alpha = 1$, we see an asymptotic or limiting behavior for the strength of the noise. Quantitatively, as α went from 2 to 1.5 (from Gaussian to Lévy distribution), there is a marked *decrease* in the magnitude of the differences; as α went from 1.5 to 1, we saw an *increase* in the magnitude of the differences.

Another finding is that uncorrelated (white) noises act very similarly, i.e., white Wiener nose had similar effects on the current as white Lévy noises, regardless of the stability-parameter α for the Lévy noises.

On the other hand, the time-correlated (colored) noises initially show a big difference at $\alpha = 2$ (Gaussian distribution), but begin to become indistinguishable as we move from $\alpha = 2$ to $\alpha = 1$ (Cauchy distribution). However, we also noted jumps developing in the plot of differences as the distribution went from Gaussian to Cauchy.

In the experiments on the period of the velocity of the shear flow, a higher-frequency flow $\frac{\omega}{3}$ showed noticeable increases in the amplitude of the oscillations or variability of the averaged scalar values, with the biggest increase seen with colored Lévy noise (almost doubled). However, this increase in diffusion is only local, and oscillatory, hence did not affect the average values for the tracer.

References

[1] Murray SP, Johns WE. Direct observations of seasonal exchange throught the Bab el Mandab Strait. Geophys Res Lett 1997;24:2557–60.
[2] Dijkstra HA. Nonlinear physical oceanography. Boston: Kluwer Academic Publishers; 2000.
[3] Alos E, Bonaccorsi S. Stability for SPDEs with Dirichlet white-noise boundary conditions. Infin Dimens Anal Quantum Probab Relat Top 2002;5:465–81.
[4] Da Prato G, Zabczyk J. Evolution equations with white-noise boundary conditions. Stochast Stochast Rep 1993;42:167–82.
[5] Freidlin MI, Wentzell AD. Reaction–diffusion equations with randomly perturbed boundary conditions. Ann Prob 1992;20:963–86.
[6] Sowers RB. Multidimensional reaction–diffusion equations with white noise boundary perturbations. Ann Prob 1994;22:2071–121.
[7] Artale V, Calmanti S, Sutera A. Thermohaline circulation sensitivity to intermediate-level anomalies. Tellus 2002;54A:159–74.
[8] Kloeden PE, Platen E. Numerical solution of stochastic differential equations. Berlin: Springer-Verlag; 1999.
[9] Wolpert RL. In: El-Shaarawi AH, Piegorsch WW, editors. Lévy Processes (Encyclopedia of Environmetrics). Chichester, NY: John Wiley and Sons; 2002.
[10] Woyczynski WA. In: Mikosch T, Barndorff-Nielsen O, Resnick S, editors. Lévy processes in the physical sciences (Lévy processes – theory and applications). Boston: Birkhäuser; 2001. p. 241–66.
[11] Young WR, Rhines PB, Garrett CJR. Shear-flow dispersion, internal waves and horizontal mixing in the ocean. J Phys Oceanogr 1982;12:515–27.
[12] Özgökmen TM, Fischer PF, Duan J, Iliescu T. Three-dimensional turbulent bottom density currents from a high-order nonhydrostatic spectral element model. J Phys Oceanogr 2004;34:2006–26.
[13] Boñgolan-WalshVP, Duan J, Fischer PF, Özgökmen T, Iliescu T. Impact of boundary conditions on entrainment and transport in gravity currents. J Appl Math Modell, Elsevier, in preparation.
[14] Applebaum D. Lévy processes and stochastic calculus. Cambridge: Cambridge University Press; 2004.
[15] Janicki A, Weron A. Simulation and chaotic behavior of alpha-stable stochastic processes. New York: Marcel Dekker, Inc.; 1994.
[16] Kunita H. In: Rao MM, editor. Stochastic differential equations based on Lévy processes and stochastic flows of diffeomorphisms in new perspectives (trends in mathematics). Berlin: Birkhäuser; 2004.

UNCORRECTED PROOF

Please cite this article in press as: Boñgolan-Walsh VP et al., Dynamics of transport under random fluxes on the boundary, Commun Nonlinear Sci Numer Simul (2007), doi:10.1016/j.cnsns.2006.09.019